Valley-Polarized Interlayer Conduction of Anisotropic Dirac Fermions in $SrMnBi_2$

Y. J. Jo,[1,*] Joonbum Park,[2] G. Lee,[3] Man Jin Eom,[2] E. S. Choi,[4] Ji Hoon Shim,[3] W. Kang,[5] and Jun Sung Kim[2,†]
[1]*Department of Physics, Kyungpook National University, Daegu 702-710, Korea*
[2]*Department of Physics, Pohang University of Science and Technology, Pohang 790-784, Korea*
[3]*Department of Chemistry, Pohang University of Science and Technology, Pohang 790-784, Korea*
[4]*National High Magnetic field Laboratory, Florida State University, Tallahassee, Florida 32310, USA*
[5]*Department of Physics, Ewha Womans University, Seoul 120-750, Korea*
(Received 6 January 2014; published 6 October 2014)

We report the valley-selective interlayer conduction of $SrMnBi_2$ under in-plane magnetic fields. The c-axis resistivity of $SrMnBi_2$ shows clear angular magnetoresistance oscillations indicating coherent interlayer conduction. Strong fourfold variation of the coherent peak in the c-axis resistivity reveals that the contribution of each Dirac valley is significantly modulated by the in-plane field orientation. This originates from anisotropic Dirac Fermi surfaces with strong disparity in the momentum-dependent interlayer coupling. Furthermore, we found a signature of broken valley symmetry at high magnetic fields. These findings demonstrate that a quasi-two-dimensional anisotropic Dirac system can host a valley-polarized interlayer current through magnetic valley control.

DOI: 10.1103/PhysRevLett.113.156602 PACS numbers: 72.15.-v, 71.18.+y, 75.47.-m

Controlling the valley degree of freedom can be an effective way to modulate charge conduction and to induce intriguing phases [1–10]. In the so-called Dirac materials like graphene, two energy bands, corresponding to two equivalent sublattices, intersect linearly at different positions in the momentum space, providing multiple valley degeneracy. Since the valley degeneracy is balanced by crystal symmetry, producing a valley-selective current usually requires breaking crystal symmetry by, e.g., strain [1–3]. However, a recent study on a three-dimensional (3D) Dirac material, bismuth, demonstrated that a rotating magnetic field modulates the contribution of each valley to the conduction and also reveals the field-induced valley polarization [7–9]. In this case, the essential ingredient for magnetic valley control is the strong anisotropy in the Dirac valleys, which has been rarely found in the Dirac materials.

Among various Dirac materials, $SrMnBi_2$ is of particular interest because of its highly anisotropic quasi-two-dimensional (2D) Fermi surface (FS) [11–15]. In $SrMnBi_2$, four valley-degenerate Dirac cones are on the Γ-M symmetry lines in the Brillouin zone, which has distinct energy dispersion against the momentum direction. Along the Γ-M line, a significant overlap between Bi $p_{x,y}$ orbitals in the plane leads to fast dispersion. On the other hand, much slower dispersion normal to the Γ-M line is due to hybridization between Sr $d_{xz,yz}$ and Bi $p_{x,y}$ orbitals. The resulting anisotropy in the Fermi velocity of the Dirac cone reaches ~5–10 [11,12,15], much larger than found in other Dirac systems [16,17]. Therefore, $SrMnBi_2$ provides a model system with anisotropic quasi-2D Dirac valleys, which can host the valley-polarized current under a magnetic field.

In this Letter, we report that the interlayer conduction of $SrMnBi_2$ can indeed be valley polarized at a tilted magnetic field. From a detailed investigation of angular magnetoresistance oscillations (AMROs), we found that the contribution of each valley to the interlayer conduction strongly depends on the in-plane field direction. In contrast to bismuth, the valley control in $SrMnBi_2$ is based on the field-induced change in the coherent interlayer conduction, which is sensitive to the curvature of the side wall of the quasi-2D FS. The resulting anisotropy is significantly enhanced at high magnetic fields, reaching ~100 without saturation, much higher than found in bismuth. Furthermore, we found a signature of broken valley degeneracy at high magnetic fields. These results suggest that the valley degree of freedom in quasi-2D anisotropic Dirac systems can be effectively controlled by the in-plane magnetic field.

The temperature dependence of the in-plane (ρ_{ab}) and the out-of-plane (ρ_c) resistivity of $SrMnBi_2$ is shown in Fig. 1(b). Experimental details are given in Supplemental Material [18]. In the whole temperature range, $\rho_c(T)$ is nearly 2 orders of magnitude larger than $\rho_{ab}(T)$. A broad maximum at $T \sim 200$ K in $\rho_c(T)$ resembles the typical behavior of quasi-2D systems showing a crossover from high-T incoherent to low-T coherent conduction [19,20]. Previous studies [11,12] revealed quasi-2D open FSs and a 3D closed FS with a donut shape in the Brillouin zone [Fig. 1(a)], which are denoted as α and β FSs, respectively [21]. In such a multiband system, the c-axis conduction is often dominated by the 3D FS. However, the T dependence of ρ_c and its field dependence shown below suggest that quasi-2D FSs significantly contribute to interlayer conduction in $SrMnBi_2$.

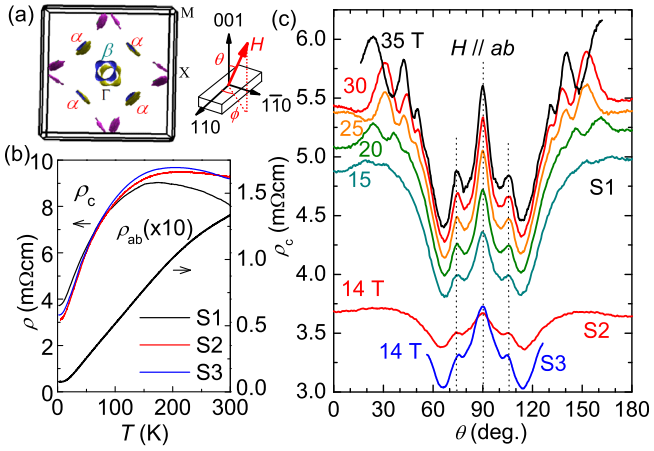

FIG. 1 (color online). (a) Calculated Fermi surface of $SrMnBi_2$. The quasi-2D Dirac FSs and the 3D FS near Γ are denoted by α_n (n = valley index) and β, respectively. Also the definition of polar (θ) and azimuthal (ϕ) angles is shown. (b) Temperature dependence of the in-plane resistivity (ρ_{ab}) of $S1$ and the c-axis resistivity (ρ_c) of $S1$, $S2$, and $S3$. (c) The $\rho_c(\theta)$ for $S1$ at $T = 0.6$ K under various magnetic fields up to $H = 35$ T. The $\rho_c(\theta)$ curves for $S2$ and $S3$ taken at $H = 14$ T and $T = 2$ K are also shown. The azimuthal angle is fixed at $\phi = 30°$. The coherent peak at $\theta = 90°$ as well as Yamaji peaks at $\theta = 75°$ and 105° are indicated by the dashed lines.

The c-axis magnetoresistivity ρ_c at tilted magnetic fields exhibits clear AMRO behaviors for all three samples. The definition of the polar (θ) and azimuthal (ϕ) angles of the magnetic field is given in Fig. 1(a), and here the azimuthal angle is fixed at $\phi = 30°$. Near $H\|c$ ($\theta = 0$ or 180°), the peak positions of the AMRO depend strongly on the field strength as shown for $S1$ in Fig. 1(c). This AMRO originates from the Shubnikov–de Haas (SdH) effect. The AMRO curves taken at different fields up to 35 T fall onto a single curve, when plotted against the normal component of the magnetic field $H_\perp = H\cos\theta$ [18]. This indicates that the responsible FS for the SdH oscillations is 2D, which corresponds to the α FS in Fig. 1(a). The SdH frequency $F = 127(3)$ T is in good agreement with the size of the α FS with $F = 137(7)$ T, estimated from the in-plane magnetoresistance [14].

There are additional peaks near $H\|ab$, whose positions are not sensitive to the field strength. This AMRO near $H\|ab$ arises from the geometrical effect of the quasi-2D FS. At characteristic angles, called Yamaji angles, the quasi-2D FS has only one extremal cross section, and the group velocity along the c axis is averaged to zero in the orbits, producing the resistive peaks [22–24]. Furthermore, the resistive peak is also found with the in-plane H at $\theta = 90°$. The width of the 90° peak, estimated from the derivatives of $\rho_c(\theta)$, is independent of the field strength up to 35 T [18]. This confirms that the 90° peak is the coherent peak, which is attributed to the effect of either the closed orbits [23–25] or the self-crossing orbits [26] formed on the side of the corrugated quasi-2D FS. These results clearly show that the coherent conduction in the quasi-2D α FSs contributes significantly to the c-axis conduction in $SrMnBi_2$.

Figure 2 presents the normalized c-axis resistivity $\rho_c(\theta)/\rho_c(\theta = 0)$ as a function of the polar angle (θ) at different azimuthal angles (ϕ). The AMRO curves taken at different magnetic fields [Fig. 2(a)] and temperatures [Fig. 2(b)] are offset for clarity. The magnitude of the coherent peak shows a clear ϕ dependence even at high T or at low H. At a certain ϕ, like $\phi = 90°$, the coherent peak is almost completely suppressed. At low T or high H, Yamaji peaks develop, whose positions are systematically modified by changing ϕ [Fig. 2(d)]. The momentum $k_\parallel(\phi)$, the maximum Fermi wave-vector projection on the plane of rotation of the field, is estimated from the Yamaji peaks [18]. The strong fourfold variation of $k_\parallel(\phi)$ [Fig. 2(c)] can be attributed to two 90°-rotated FSs having an elliptical cross section. Based on the relation $k_\parallel(\phi)^2 = [k_F^{\max}\cos(\phi)]^2 + [k_F^{\min}\sin(\phi)]^2$ [27], where $k_F^{\max}$ ($k_F^{\min}$) is the longer (shorter) radius for the ellipse, we calculated the $k_\parallel(\phi)$ curve by using the FS size $A_k = 1.21$ nm^{-2} from the SdH frequency of 127(3) T and the anisotropy $k_F^{\max}/k_F^{\min} \approx 6$ [11,15] as shown in Fig. 2(c). A good agreement between the experiment and calculation confirms that the relevant FS for the AMRO is indeed the highly anisotropic α FS. This clearly demonstrates that the variation of the coherent peak due to the geometrical effect of the quasi-2D α FS

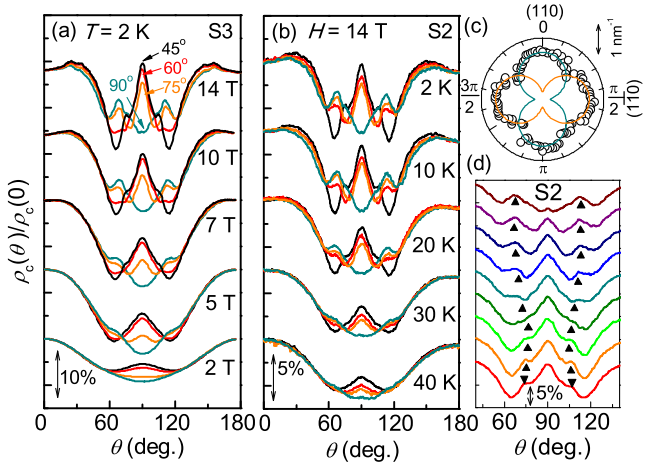

FIG. 2 (color online). (a) The normalized resistivity $\rho_c(\theta)/\rho_c(0)$ for $S3$ taken at $T = 2$ K with different azimuthal angles (ϕ) and magnetic fields. (b) The normalized $\rho_c(\theta)/\rho_c(0)$ for $S2$ taken at $H = 14$ T with different ϕ and temperatures. In (a) and (b), the data are shifted along the vertical axis for clarity, and the same color code for ϕ is used. (c) The projection vector ($k_\parallel$) estimated from Yamaji peaks. The solid lines are the calculated curve using two 90°-rotated elliptical quasi-2D FSs (see the text). (d) The systematic changes in $\rho_c(\theta)/\rho_c(0)$ of $S2$, taken at $H = 14$ T and $T = 2$ K, for different ϕ from 80° (top) to 32° (bottom) with a span of 6°. The curves are offset for clarity, and the small triangles indicate the position of the Yamaji peaks.

determines the significant ϕ dependence of $\rho_c(\phi)$ at $\theta = 90°$ [28].

The $\rho_c(\theta = 90°, \phi)$ at the coherent peak exhibits strong fourfold symmetry in the ϕ dependence [Figs. 3(a) and 3(b)]. With increasing H, the anisotropy of $\rho_c(\phi)$ becomes stronger; i.e., the dips at $\phi = m\pi/2$ (m = integer) become deeper and narrower. This reflects strong twofold anisotropy in the contribution of each α FS, which is rotated by 90° against its neighbors [Fig. 1(a)], consistent with the results in Fig. 2(c). The strong twofold anisotropy of a single α FS originates from the field-induced change in the interlayer conduction. At high in-plane H, conduction electrons of the quasi-2D FS make complete closed orbits before scattering by the Lorentz force $F_L \propto v_F \times B$, significantly reducing the interlayer conduction. However, this is not the case for electrons on the flat part of the FS, which experience nearly zero F_L due to the almost parallel v_F to B. Therefore, the c-axis conductivity under the in-plane magnetic field is extremely sensitive to the curvature of the side wall of the FS, as found in various quasi-2D systems [29–31].

In $SrMnBi_2$, when the magnetic field is along the longer axis of the α FS ($H \perp \Gamma$-M), large corrugation on the side of the FS leads to the minimum conductivity $\sigma_c(\phi)$. In contrast, for the magnetic field along the shorter axis ($H \| \Gamma$-M), electrons in the flat side FS have the maximum σ_c [Fig. 3(c)]. The alternative explanation with the self-crossing orbits [26] predicts the same angle dependence of $\sigma_c(\phi)$. As a consequence, the rotating field by 90° turns on or off the contribution of a single α FS to the conduction [Fig. 3(d)]. Here, four valley-degenerate anisotropic α FSs, denoted by valley index n, are rotated by 90° [Fig. 1(a)]. Then the ϕ dependence of c-axis conduction from the valleys with odd indices ($n = 1$ and 3) is shifted by 90° against that from the valleys of even indices ($n = 2$ and 4) [Fig. 3(e)]. In other words, when the valleys with odd n contribute the most to the c-axis conduction, the valleys with even n do the least. Hence, the in-plane field orientation can control the relative contribution of the valleys with odd or even indices in $SrMnBi_2$.

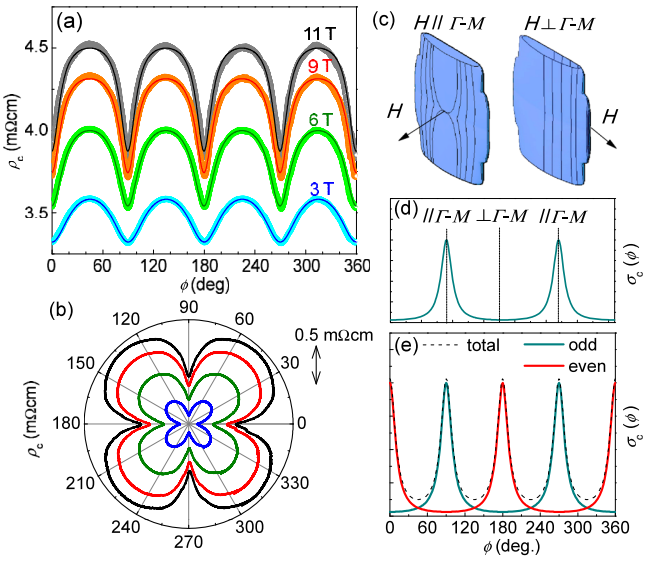

FIG. 3 (color online). (a) The azimuthal angle (ϕ) dependence of the c-axis resistivity $\rho_c(\phi)$ of $S1$ under various magnetic fields ($\theta = 90°$) at $T = 5$ K. The solid lines are the fit of the model taking account of the anisotropic valley conduction (see the text). (b) The corresponding polar plot for $\rho_c(\phi)$. (c) Schematic illustration of the quasi-2D α FS with H along or normal to the Γ-M symmetry line in the k space. The electron orbits formed perpendicular to the magnetic field are shown in both cases. (d) The expected twofold ϕ-dependent conductivity $\sigma_c(\phi)$ from a single Dirac valley (α FS). (e) Each contribution from the valleys with odd and even index (solid lines) together with the total conductivity (dashed line).

In order to estimate the twofold anisotropy in the α FS, we employed a phenomenological model for $\rho_c(\phi)$ taking account of contribution from the valley-degenerate α FS and the 3D β FS [32]. Here we assumed that the conductivity of β FS (σ_β) has negligible ϕ dependence, which is justified by the fact that the ϕ dependence of $\rho_c(\phi)$ at $\theta = 90°$ is dominated by the variation of the coherent peak [Fig. 2]. For the twofold anisotropic interlayer conductivity of each α FS [$\sigma_{\alpha,n}(\phi)$], a phase shift by 90° is introduced between those of odd and even n. Then, the c-axis conductivity $\sigma_c(\phi) \approx \rho_c^{-1}(\phi)$ [33] is approximately given as their sum, expressed by

$$\sigma_c(\phi) = \sum_{n=1}^{4} \sigma_{\alpha,n}(\phi) + \sigma_\beta = \frac{2\sigma_{2D}}{1 + r\cos^2\phi} + \frac{2\sigma_{2D}}{1 + r\cos^2(\phi + \pi/2)} + \sigma_{3D}, \quad (1)$$

where the σ_{2D} (σ_{3D}) are the relative contribution of the α (β) FS and the anisotropy factor r reflects the anisotropy in effective mass and scattering time. This model nicely reproduces the observed data [Fig. 3(a)]. The fit yields the ratio between the quasi-2D (four α FSs) and 3D (β FS) conductivities, $4\sigma_{2D}/\sigma_{3D} \sim 0.08$, suggesting the α FSs contributes ~10% of the total c-axis conduction. This is consistent with the fact that the amplitude of the SdH oscillations from the α FSs is ~10% of ρ_c [Fig. 1(c)].

Despite many similarities, as compared to bismuth [7], the quasi-2D nature of $SrMnBi_2$ leads to different high-field dependence of the resistive anisotropy $r(H)$. As shown in Fig. 4(a), the dips in $\rho_c(\phi)$ become narrower with H, indicating a monotonic increase of $r(H)$ [33]. At low temperatures, the resistive anisotropic factor $r(H)$ increases linearly with H but starts to bend above $H \sim 14$ T, reaching ~100 at $H = 30$ T [Fig. 4(b)]. This contrasts to the case of bismuth [7], showing saturation of $r(H)$ to its high-field limit ~40, mainly set by the anisotropy in the effective mass of 3D FSs. In quasi-2D systems, field-induced suppression of the interlayer

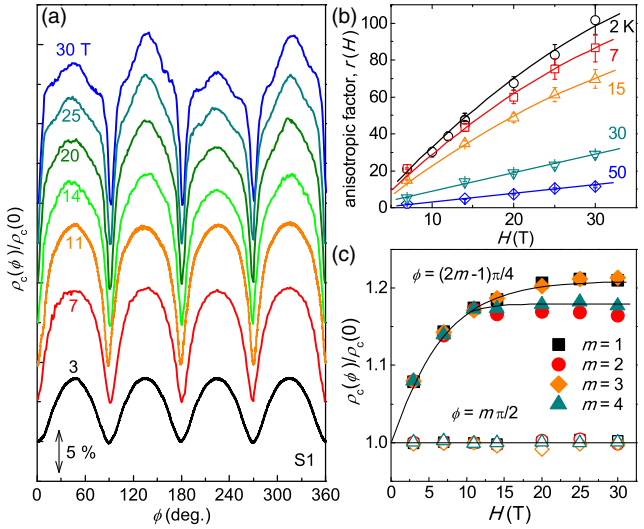

FIG. 4 (color online). (a) The ϕ dependence of the normalized $\rho_c(\phi)/\rho_c(\phi = 0)$ of $S1$ at high fields up to $H = 30$ T at $T = 2$ K. (b) The field dependence of the anisotropic factor $r(H)$ for the α FS. (c) The field dependence of $\rho_c(\phi)/\rho_c(\phi = 0)$ for the peaks at $\phi = (2m-1)\pi/4$ and for the dips at $\phi = m\pi/2$ $(m = 1, 2, 3, 4)$. The solid lines in (b) and (c) are guides to the eye.

conduction is amplified differently, depending on the corrugation of the quasi-2D FS. With increasing H along the corrugated region, a larger area of the FS does not participate in charge conduction, significantly enhancing ρ_c. On the other hand, along the flat FS, the magnetic field remains less effective in ρ_c. This leads to a much larger enhancement of $r(H)$ at high H in $SrMnBi_2$ [34]. Therefore, valley control in the interlayer conduction can be more effective in quasi-2D Dirac systems [35].

In quasi-2D Dirac systems, strong anisotropic corrugation of the FS is essential for valley control. In $SrMnBi_2$, the relevant states along the shorter axis of the α FS are the Bi $p_{x,y}$ orbitals lying in the Bi plane. Their significant overlap in the plane gives fast dispersion and a strong 2D character. In contrast, along the larger axis of the α FS, hybridization between the Bi p and Sr d orbitals in the neighboring layers leads to much slower dispersion and a relatively stronger 3D character. The strong disparity in the interlayer coupling and the curvature of the in-plane FS cross section of the α FS are intimately related with each other in $SrMnBi_2$. This implies that further tuning of the orbital overlap by, e.g., external pressure or chemical substitution can enhance the anisotropic factor r for more effective valley control.

Finally, we discuss possible broken fourfold symmetry in $\rho_c(\phi)$ at high fields. As shown in Fig. 4(a), the fourfold symmetry in $\rho_c(\phi)$, clearly present at low H, is destroyed above $H \sim 14$ T, where the $r(H)$ deviates from the H-linear dependence [Fig. 4(b)]. From the two-axis rotation measurements at $H = 14$ T, we found a somewhat weaker difference between the coherent peaks than found in Fig. 4(a), indicating a possible misalignment of the field out of the ab plane. However, the difference between the $\rho_c(\phi)$ data taken at $\phi = 45°$ (225°) and at $\phi = 135°$ (315°) remains negligible below $H \sim 14$ T and suddenly becomes significant at higher fields [Fig. 4(c)]. Also, the $\rho_c(\phi)$ for $\phi = (2m-1)\pi/4$ shows twofold behavior, whereas data taken at $\phi = m\pi/2$ $(m = 1, 2, 3, 4)$ remain symmetric at high magnetic fields [36]. Furthermore, the two-axis rotation measurements on another sample $S3$ show a weak but noticeable twofold behavior at $H = 14$ T [18]. These results cannot be explained by the field misalignment only. In fact, similar behavior of broken valley degeneracy was found in bismuth at high magnetic fields [7,9]. In $SrMnBi_2$, incipient electronic instability might be stabilized at high fields, lifting valley degeneracy. The nesting effect of the flat part of the α FSs can be important for electronic instability, which also induces a charge density wave phase in structurally related compounds $CaMnBi_2$ and $LaAgBi_2$ [37–40]. Further investigation at high fields is highly desirable to clarify the possible electronic nematic phase. Nevertheless, our findings suggest that interlayer conduction of anisotropic quasi-2D Dirac systems can be modulated with a magnetic field, providing an effective way for valley control.

In conclusion, we have shown that the coherent interlayer conduction of a quasi-2D Dirac system $SrMnBi_2$ is significantly modulated by a rotating magnetic field. Based on the detailed AMRO experiments, we found that such a strong modulation of the c-axis resistivity is attributed to the magnetically valley-selective conduction. The key ingredient of magnetic valley control in $SrMnBi_2$ is strong momentum-dependent disparity in interlayer coupling. The layered compounds with anisotropic Dirac valleys provide an interesting platform to study valley-selective conduction and also field-induced valley polarization at high magnetic fields.

The authors thank I. Mazin and L. Boeri for fruitful discussion. This work was supported by National Research Funding (NRF) through the BSR (Grants No. 2012-013838 and No. 2013R1A1A2063904), SRC (Grant No. 2011-0030785), the Max Planck POSTECH/KOREA Research Initiative Program (Grant No. 2011-0031558), and also by Institute for Basic Science (IBS). W. K. was supported by the NRF (Grants No. 2008-0061893 and No. 2010-00453). A portion of this work was performed at the NHMFL, supported by National Science Foundation Cooperative Agreement No. DMR-1157490, the State of Florida, and the U.S. Department of Energy.

*jophy@knu.ac.kr
†js.kim@postech.ac.kr

[1] O. Gunawan, Y. P. Shkolnikov, K. Vakili, T. Gokmen, E. P. De Poortere, and M. Shayegan, Phys. Rev. Lett. **97**, 186404 (2006).

[2] N. C. Bishop, M. Padmanabhan, K. Vakili, Y. P. Shkolnikov, E. P. De Poortere, and M. Shayegan, Phys. Rev. Lett. **98**, 266404 (2007).

[3] O. Gunawan, T. Gokmen, K. Vakili, M. Padmanabhan, E. P. De Poortere, and M. Shayegan, Nat. Phys. **3**, 388 (2007).

[4] K. Takashina, Y. Ono, A. Fujiwara, Y. Takahashi, and Y. Hirayama, Phys. Rev. Lett. **96**, 236801 (2006).

[5] D. Xiao, W. Yao, and Q. Niu, Phys. Rev. Lett. **99**, 236809 (2007).

[6] K. F. Mak, K. He, J. Shan, and T. F. Heinz, Nat. Nanotechnol. **7**, 494 (2012).

[7] Z. Zhu, A. Collaudin, B. Fauque, W. Kang, and K. Behnia, Nat. Phys. **8**, 89 (2012).

[8] A. Popescu and L. M. Woods, Adv. Funct. Mater. **22**, 3945 (2012).

[9] R. Küchler, L. Steinke, R. Daou, M. Brando, K. Behnia, and F. Steglich, Nat. Mater. **13**, 461 (2014).

[10] D. A. Abanin, S. A. Parameswaran, S. A. Kivelson, and S. L. Sondhi, Phys. Rev. B **82**, 035428 (2010).

[11] J. Park *et al.*, Phys. Rev. Lett. **107**, 126402 (2011).

[12] G. Lee, M. A. Farhan, J. S. Kim, and J. H. Shim, Phys. Rev. B **87**, 245104 (2013).

[13] J. K. Wang, L. L. Zhao, Q. Yin, G. Kotliar, M. S. Kim, M. C. Aronson, and E. Morosan, Phys. Rev. B **84**, 064428 (2011).

[14] K. Wang, D. Graf, H. Lei, S. W. Tozer, and C. Petrovic, Phys. Rev. B **84**, 220401 (2011).

[15] Y. Feng *et al.*, Sci. Rep. **4**, 5385 (2014).

[16] A. Kobayashi, S. Katayama, K. Noguchi, and Y. Suzumura, J. Phys. Soc. Jpn. **73**, 3135 (2004).

[17] P. Richard *et al.*, Phys. Rev. Lett. **104**, 137001 (2010).

[18] See Supplemental Material at http://link.aps.org/supplemental/10.1103/PhysRevLett.113.156602 for additional information regarding analysis on the AMRO of $SrMnBi_2$.

[19] T. Valla *et al.*, Nature (London) **417**, 627 (2002).

[20] D. B. Gutman and D. L. Maslov, Phys. Rev. Lett. **99**, 196602 (2007); Phys. Rev. B **77**, 035115 (2008), and references therein.

[21] The recent angle-resolved photoemission spectroscopy studies in Refs. [11,15] show the absence of the FSs near the X point. Thus we do not take into account their contribution in the c-axis conduction.

[22] K. Yamaji, J. Phys. Soc. Jpn. **58**, 1520 (1989).

[23] N. Hanasaki, S. Kagoshima, T. Hasegawa, T. Osada, and N. Miura, Phys. Rev. B **57**, 1336 (1998).

[24] R. H. McKenzie and P. Moses, Phys. Rev. Lett. **81**, 4492 (1998); P. Moses and R. H. McKenzie, Phys. Rev. B **60**, 7998 (1999); M. P. Kennett and R. H. McKenzie, Phys. Rev. B **78**, 024506 (2008).

[25] T. Kawamoto, T. Mori, D. Graf, J. S. Brooks, Y. Takahide, S. Uji, T. Shirahata, and T. Imakubo, Phys. Rev. Lett. **109**, 147005 (2012).

[26] V. G. Peschansky and M. V. Kartsovnik, Phys. Rev. B **60**, 11207 (1999); M. V. Kartsovnik, Chem. Rev. **104**, 5737 (2004).

[27] A. House, N. Harrison, S. Blundell, I. Deckers, J. Singleton, F. Herlach, W. Hayes, J. Perenboom, M. Kurmoo, and P. Day, Phys. Rev. B **53**, 9127 (1996).

[28] The contribution from the 3D β FS may introduce the change of the monotonic background in ρ_c, which appears to be much weaker than the variation of the coherent peak [Figs. 2(a) and 2(b)].

[29] M. Kimata *et al.*, Phys. Rev. Lett. **105**, 246403 (2010).

[30] E. Ohmichi, H. Adachi, Y. Mori, Y. Maeno, T. Ishiguro, and T. Oguchi, Phys. Rev. B **59**, 7263 (1999).

[31] H. Takatsu, J. J. Ishikawa, S. Yonezawa, H. Yoshino, T. Shishidou, T. Oguchi, K. Murata, and Y. Maeno, Phys. Rev. Lett. **111**, 056601 (2013).

[32] A similar model successfully describes the valley-anisotropic conduction of bulk bismuth in Ref. [7].

[33] The presence of the 3D β FS or the off-diagonal term in σ_c is considered to be negligible for determining the ϕ dependence of $\rho_c(\phi)$. Also, σ_{3D} show a conventional monotonic decrease with H.

[34] Giant anisotropic MR has also been observed in $PdCoO_2$ (Ref. [31]), where the flat and corrugated regions coexist in a single quasi-2D FS.

[35] Because of the 3D β FS, the relative valley-polarized contribution to the total conduction remains $\sim$10% in $SrMnBi_2$, which can be further enhanced by reducing the contribution of the 3D β FS with tuning of the chemical potential or lattice structures.

[36] The ρ_c shows a 90° peak for $\phi = (2n-1)\pi/4$, whereas it shows a 90° dip for $\phi = n\pi/2$ [Figs. 2(a) and 2(b)]. Since their sharpness is comparable, the misalignment, if any, should affect the $\rho_c(\phi)$ similarly at both peaks and dips.

[37] J. B. He, D. M. Wang, and G. F. Chen, Appl. Phys. Lett. **100**, 112405 (2012).

[38] K. Wang, D. Graf, L. Wang, H. Lei, S. W. Tozer, and C. Petrovic, Phys. Rev. B **85**, 041101 (2012).

[39] K. Wang, D. Graf, and C. Petrovic, Phys. Rev. B **87**, 235101 (2013).

[40] We note that the antiferromagnetic Mn layer may also play a role for stabilizing the broken symmetry behavior.